



Polar plot maps by parametric strain echocardiography allow accurate evaluation of non-viable transmural scar tissue in ischaemic heart disease

Donato Mele^{1*}, Andrea Fiorencis¹, Elisabetta Chiodi², Chiara Gardini¹, Giorgio Benea², and Roberto Ferrari³

¹Cardiology Unit, Azienda Ospedaliero-Universitaria, Via Aldo Moro 8, Cona, 44124 Ferrara, Italy; ²Radiology Unit, Azienda Ospedaliero-Universitaria, Ferrara, Italy; and ³Department of Cardiology and LTTA Centre, University Hospital of Ferrara and Maria Cecilia Hospital, GVM Care & Research, E.S. Health Science Foundation, Cotignola, Italy

Received 7 March 2015; accepted after revision 6 July 2015

Aims

Assessment of left ventricular (LV) transmural scar tissue in clinical practice is still challenging because magnetic resonance imaging (MRI) and nuclear techniques have limited access and cannot be performed extensively. The aim of this study was to verify whether parametric two-dimensional speckle-tracking echocardiography (2D-STE) can more accurately localize and quantify LV transmural scar tissue in patients with healed myocardial infarct (MI) in comparison with MRI.

Methods and results

Thirty-one consecutive patients (age 56 ± 32 years, 29 males) with MRI and echocardiography performed after at least 6 months from an acute MI were studied. Apical LV longitudinal strain images by 2D-STE and short-axis contrast images by MRI were analysed to generate parametric bull's eye maps showing the distribution of the LV transmural scar tissue, whose extension was measured by planimetry and expressed as a percentage of the total myocardial area. Twelve patients also had early 2D-STE and MRI examinations after the acute MI. 2D-STE accurately quantified the extent of transmural scar tissue vs. MRI ($r = 0.86$; limits of agreement 10.0 and -9.5%). Concordance between 2D-STE and MRI for transmural scar tissue localization was high, with only 3.6% of discordant segments using an LV 16-segment model. Lin coefficients, intra-class correlation coefficients, and Bland–Altman analysis showed very good intra- and inter-observer reproducibility for 2D-STE evaluations. The transmural scar tissue area at 6 months could be predicted by early 2D-STE evaluation.

Conclusion

2D-STE polar plots of LV longitudinal strain characterize transmural scar tissue accurately compared with MRI and may facilitate its assessment in clinical practice.

Keywords

Speckle-tracking echocardiography • Strain • Myocardial infarct • Transmural scar

Introduction

Evaluation of presence, localization, and extent of left ventricular (LV) transmural scar tissue in patients with ischaemic heart disease is of fundamental importance in clinical practice. For example, since transmural scar myocardial segments do not recover from their loss of contractile function, the absence of viability affects the decision to perform a revascularization.¹ In recent years, two-dimensional speckle-tracking echocardiography (2D-STE) has been used to

recognize transmural infarct scar tissue using analysis of longitudinal, circumferential, and radial myocardial deformation.^{2–5} However, studies based on 2D-STE focused mainly on analysis of strain curves and did not evaluate the value of parametric strain polar maps for a comprehensive assessment of the area size and topographic distribution of the transmural scar.

The primary aim of this study was to verify whether parametric 2D-STE is accurate and reproducible in recognizing and quantifying the area of the transmural scar tissue as well as in describing its

* Corresponding author. Tel: +39 0532 239058; Fax: +39 0532 239048, E-mail address: donatomele@libero.it

Published on behalf of the European Society of Cardiology. All rights reserved. © The Author 2015. For permissions please email: journals.permissions@oup.com.

topographic localization in patients with healed LV myocardial infarct (MI) in comparison with cardiac magnetic resonance imaging (MRI). As a secondary aim, we sought to verify whether the parametric 2D-STE infarct area is better associated with the MRI transmural infarct scar size than other parameters of LV systolic function, such as global longitudinal strain (GLS) and ejection fraction (EF). Finally, in a subgroup of patients who also had the 2D-STE and MRI examinations early after the acute MI, we investigated whether the final size of the transmural infarct scar can be predicted by the early evaluation of the parametric 2D-STE infarct area.

Methods

Patient population

Patients with healed MI were selected within a 1-year period from the database of the Cardiology and Radiology Units to have: a cardiac MRI study performed after at least 6 months from a first acute ST-elevation MI; an echocardiographic examination performed within 7 days from the MRI study. Patients were excluded if they had a new coronary artery syndrome and/or additional revascularization procedures between the first myocardial event and the planned MRI and echocardiographic studies at 6 months. The acute ST-elevation MI was diagnosed on the basis of clinical presentation, electrocardiographic findings, and troponin elevation. All patients underwent a primary percutaneous coronary intervention with/without successful recanalization of the infarct-related coronary artery. Thirty-one patients fulfilled the above-mentioned criteria and were included in the study. A subgroup of 12 patients had both a cardiac MRI study performed 1 or 2 days after the primary percutaneous coronary intervention (all with successful recanalization of the infarct-related coronary artery) and an echocardiographic examination immediately before the MRI. All patients were in sinus rhythm at the moment of both the MRI and echocardiographic studies. All echocardiographic examinations were digitally stored. Patients' characteristics are reported in Table 1.

Table 1 Patient characteristics

Variable	Overall patients
Age (mean \pm SD)	56 \pm 32 years
Sex (M/F)	29/2
Body surface area (mean \pm SD)	1.96 \pm 0.2 m ²
Hypertension (n)	18 (58%)
Diabetes (n)	9 (29%)
Family history of myocardial infarction (n)	6 (19%)
Smoking (n)	13 (42%)
1-Vessel disease (n)	20 (65%)
2-Vessel disease (n)	6 (19%)
3-Vessel disease (n)	5 (16%)
MRI LV-EDV (mean \pm SD)	185 \pm 56 mL
MRI LV-ESV (mean \pm SD)	109 \pm 51 mL
MRI LV-SV (mean \pm SD)	76 \pm 18 mL
MRI LV-EF (mean \pm SD)	44 \pm 13%
LV-GLS (mean \pm SD)	-12.7 \pm 3.7%

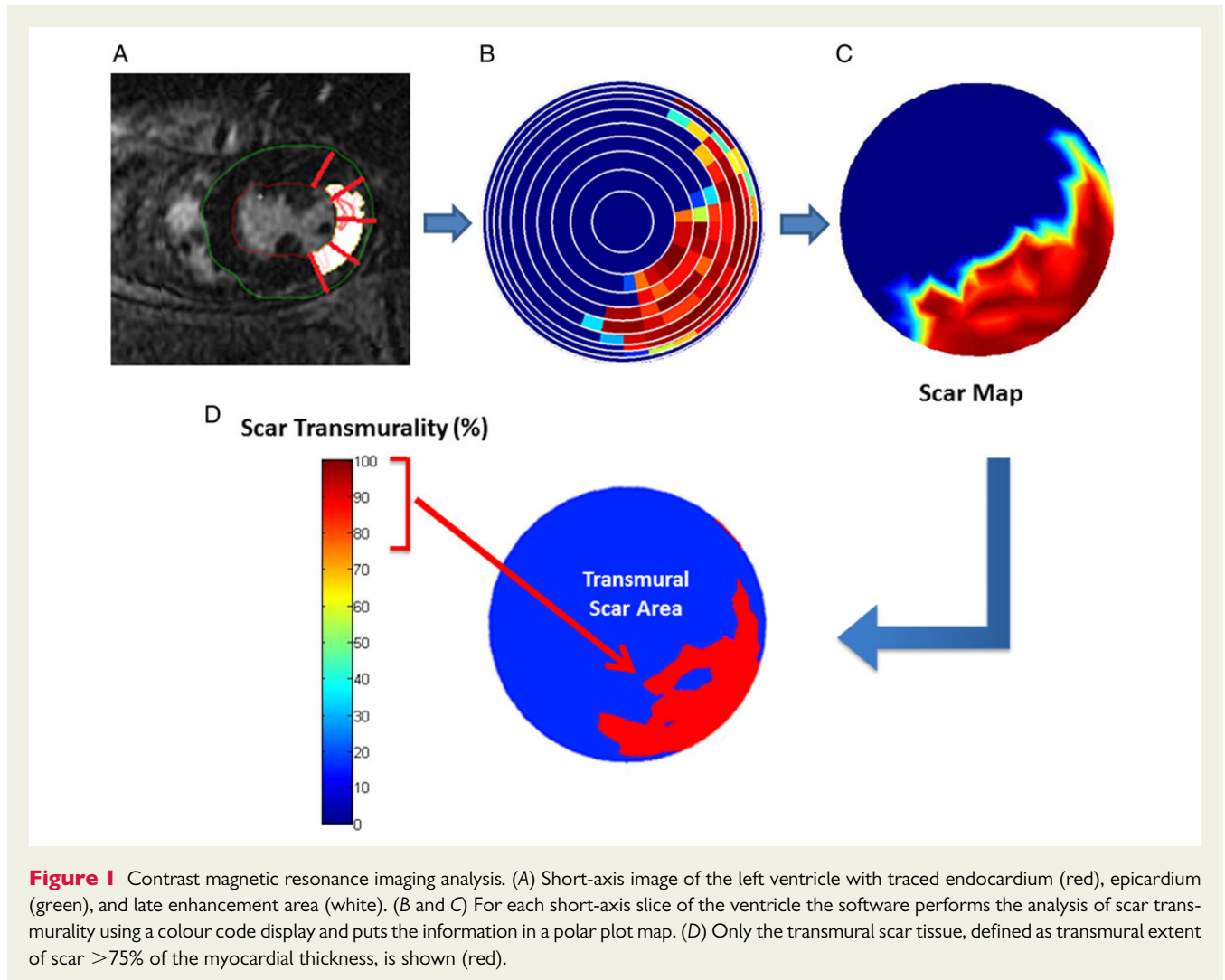
LV-EDV, left ventricular end-diastolic volume; ESV, end-systolic volume; SV, stroke volume; EF, ejection fraction; GLS, global longitudinal strain; MRI, magnetic resonance imaging; SD, standard deviation.

Magnetic resonance imaging

All images were acquired using a 1.5-T MRI system optimized for cardiovascular applications (Signa HDX, GE Medical Systems, Milwaukee, WI, USA). An 8-channel phased-array surface coil was used. Localization was performed using breath-hold single-phase steady-state free precession (SSFP) images of true anatomical axes of the heart. Subsequently, cine SSFP and delayed enhancement (DE) sequences were obtained. Cine SSFP images were acquired in short- and long-axis views. For the short-axis view sequences, a slice thickness of 10 mm with no gap in identical slice positions, covering the LV from the base to the apex, was used. The DE images (fast-gradient-echo inversion-recovery) were acquired 7–10 min after bolus intravenous injection of 0.15 mmol/kg body weight of gadolinium-diethylenetriamine penta-acetic acid (gadobutrol, Schering, Germany), followed by saline flush. The inversion time was adapted individually to null normal myocardium. In the 12 patients evaluated early after the acute MI, additional sequences for myocardial oedema were performed. In particular, T2-weighted images were acquired by encompassing the LV in the cardiac short-axis direction with a dark-blood T2-weighted short-tau inversion-recovery fast spin echo sequence. LV end-diastolic and end-systolic volumes (EDV, ESV), stroke volume (SV), and ejection fraction (EF) were calculated according to standard methods. For myocardial DE and oedema analysis, MRI images were analysed using the software Segment CMR (Medviso, Lund, Sweden).⁶ The DE and T2-weighted short-axis slices from the base to the apex were processed with this software that delineates semi-automatically the endocardium and epicardium, identifies the areas of hyperenhancement (DE images) and hyperintensity (T2-weighted images), and calculates the percentage of LV myocardial mass characterized by oedema. It also generates polar maps showing the spatial distribution of myocardial DE from the base to the apex and circumferentially as well as the percentage of DE transmurality using a colour-coded representation (Figure 1). These maps were first processed to evidence only the transmural DE (TDE), defined as a transmural extent of DE (TME) >75% of the myocardial thickness. In patients with healed MI, the TDE represents the transmural scar tissue. The TDE area was measured by planimetry and expressed as a percentage of the total myocardial area. Subsequently, the polar maps were obtained using a TME > 50% of the myocardial thickness and areas were remeasured. For the analysis of spatial concordance between MRI TDE and 2D-STE, colour-coded polar maps were also generated using a 16-segment model. In this model, an average value of TDE corresponds to each segment (segmental transmurality value).

Conventional and speckle-tracking echocardiography

In all patients, a complete transthoracic echocardiography examination was performed using commercially available ultrasound systems (Vivid 7 and E9, GE Medical Systems, Milwaukee, WI, USA) equipped with a 3.5 MHz phased-array transducer. Image and Doppler acquisitions were obtained at held end-expiration. For the 2D-STE image acquisition, sector size and depth were adjusted to achieve optimal visualization of the whole LV myocardium in the three standard apical views (4-, 2-chamber, and long-axis view) with a frame rate between 60 and 100 fps. The LV longitudinal myocardial strain was assessed using a commercially available software (EchoPAC PC, GE Medical Systems, Milwaukee, WI, USA). End-systole was defined as aortic valve closure in the apical long-axis view. The regions of interest (ROIs) were manually outlined at end-systole by marking the endocardial borders in the apical views. A manual adjustment was performed if the automated tracking was suboptimal. Peak systolic longitudinal myocardial strain was



automatically calculated throughout the myocardium for each LV apical view and reported spatially—from base to apex and circumferentially—in a polar plot map using a colour-coded parametric representation (Figure 2). Non-viable myocardial tissue was defined as a value of peak systolic longitudinal strain $\geq -5\%$, corresponding to the clear pink colour or any shade of blue colour on the polar map. The area of this severely altered strain (SAS) was determined by planimetry by using the same software and expressed as a percentage of the total myocardial area. The relative areas of myocardial tissue with peak systolic longitudinal strain $\geq -10\%$ and $\geq -15\%$ were also calculated. For the analysis of spatial concordance between non-viable SAS myocardial tissue on 2D-STE and transmural scar tissue on cardiac MRI, colour-coded polar maps were also generated using a 16-segment model of the LV. In this model, an average value of peak systolic longitudinal strain among all local acoustic markers corresponds to each segment (segmental strain value). In addition, the GLS was determined by averaging all peak systolic segmental strain values from the three standard apical views. Longitudinal peak strain values were averaged over two consecutive cardiac cycles.

To test the reproducibility of the parametric strain method, the first and a second observer blindly recalculated the SAS area of all patients 1 week after the first reading. Recalculation included a new ROI outline on the digitally stored 2D images, polar plot generation and SAS area tracing and measurement.

Statistical analysis

The continuous variables were calculated as the average value \pm the standard deviation, whereas those that were categorical were calculated as percentages. Extent of TDE areas by MRI and SAS areas by 2D-STE were compared by Student's *t*-test (mean values), Pearson's *r* correlation coefficient, and Bland–Altman analysis. The same analyses were repeated to compare other areas measured on the 2D-STE and MRI polar plots. Locations of MRI TDE areas and 2D-STE SAS areas were compared by visual assessment; also, the percentage of LV segments with TDE and SAS was compared by χ^2 analysis. The MRI TDE areas and the 2D-STE SAS areas were measured in a blinded fashion by two different readers. All measurements of the 2D-STE SAS areas were repeated by the first (AF) and a blind second observer (CG), and the intra- and inter-observer variabilities were assessed using the Lin concordance correlation coefficient, the intra-class correlation coefficient (ICC) with confidence intervals (CIs) and the Bland–Altman analysis. The 2D-STE GLS and the MRI EF values were correlated with both the MRI scar areas and the 2D-STE strain areas at 6 months using Pearson's *r* correlation coefficient. The capability of the 2D-STE SAS area and MRI TDE area at the early post-infarct evaluation to predict the late transmural scar tissue area by cardiac DE-MRI was assessed by univariate and stepwise bivariate correlation analysis. The statistical analysis was performed using MedCalc Statistical Software version

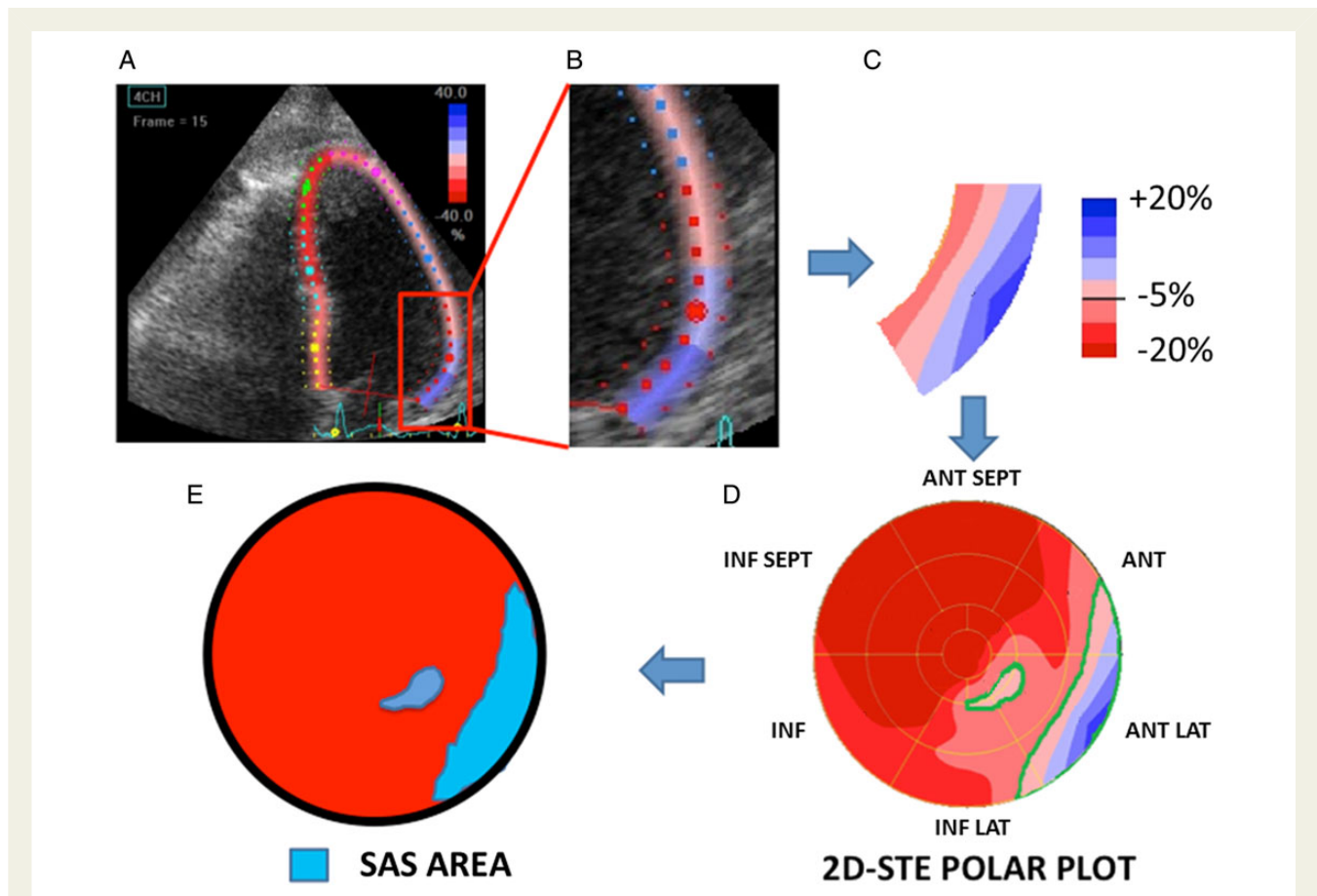


Figure 2 Two-dimensional speckle-tracking echocardiography (2D-STE) analysis. (A) Apical four-chamber view of the left ventricle with the speckle-tracking region of interest on the ventricular myocardium. (B) A portion of the lateral wall is magnified. (C and D) Strain information is used to generate a polar plot map of the ventricle. (E) Clear pink colour and all blue colours (corresponding to longitudinal strains $\geq -5\%$) are used to identify the severely altered strain (SAS) area. Ant, anterior; Lat, lateral; Inf, inferior; Sept, septum.

11.2.1.0. A P -value of <0.05 was considered statistically significant. The study was approved by the local Ethics Committee.

Results

Validation study

Transmural scar size assessment

In the 31 patients with healed MI, there was no difference between the mean 2D-STE SAS area (strain values $\geq -5\%$) and the mean MRI TDE area (TME $> 75\%$): $13.0 \pm 9.5\%$ vs. $12.8 \pm 9.0\%$, respectively ($P = 0.806$). The area values obtained using the two imaging techniques correlated well ($r = 0.86$, $P < 0.001$, Figure 3); on the Bland–Altman analysis, no bias was observed (mean difference 0.2% , $P = 0.806$ vs. 0) and all differences were within the limits of agreement (10.0 , -9.5% , Figure 3). Figure 4 illustrates some examples of SAS and TDE areas of different size obtained by 2D-STE and MRI.

Effects of different cut-off values

When the MRI scar area was defined using a TME $> 50\%$, the mean 2D-STE SAS area became different from the mean MRI area

($18.7 \pm 9.6\%$, $P < 0.001$). Although the area values obtained using the two imaging techniques correlated well ($r = 0.83$, $P < 0.001$, Figure 3), the Bland–Altman analysis showed larger errors when compared with the MRI TDE areas (mean difference -5.7% , $P < 0.001$ vs. 0 , Figure 3). When longitudinal strain values of ≥ -10 and $\geq -15\%$ were selected for analysis, the difference between the mean 2D-STE strain areas ($30.5 \pm 17.7\%$ for strain $\geq -10\%$ and $62.2 \pm 21.4\%$ for strain $\geq -15\%$) and the mean MRI areas (values reported above) was very large using both a TME of $>75\%$ ($P < 0.001$) and of $>50\%$ ($P < 0.001$). In both cases, the Bland–Altman analysis showed overestimation of the MRI scar areas (Supplementary data online, Figures S1 and S2).

Concordance of transmural scar location

Location of the transmural infarct area on the TDE MRI plots varied and all coronary territories were represented in different patients. By visual analysis, localization of SAS on 2D-STE polar plots agreed with that of TDE on MRI plots in all the 31 study patients (Figure 4). Using the 16-segment model, the percentage of LV segments with SAS on 2D-STE was 14% and that of segments with TDE on cardiac MRI was 12% ($P = 0.344$). 2D-STE and DE-MRI were concordant in recognizing the location of the LV segments with non-viable

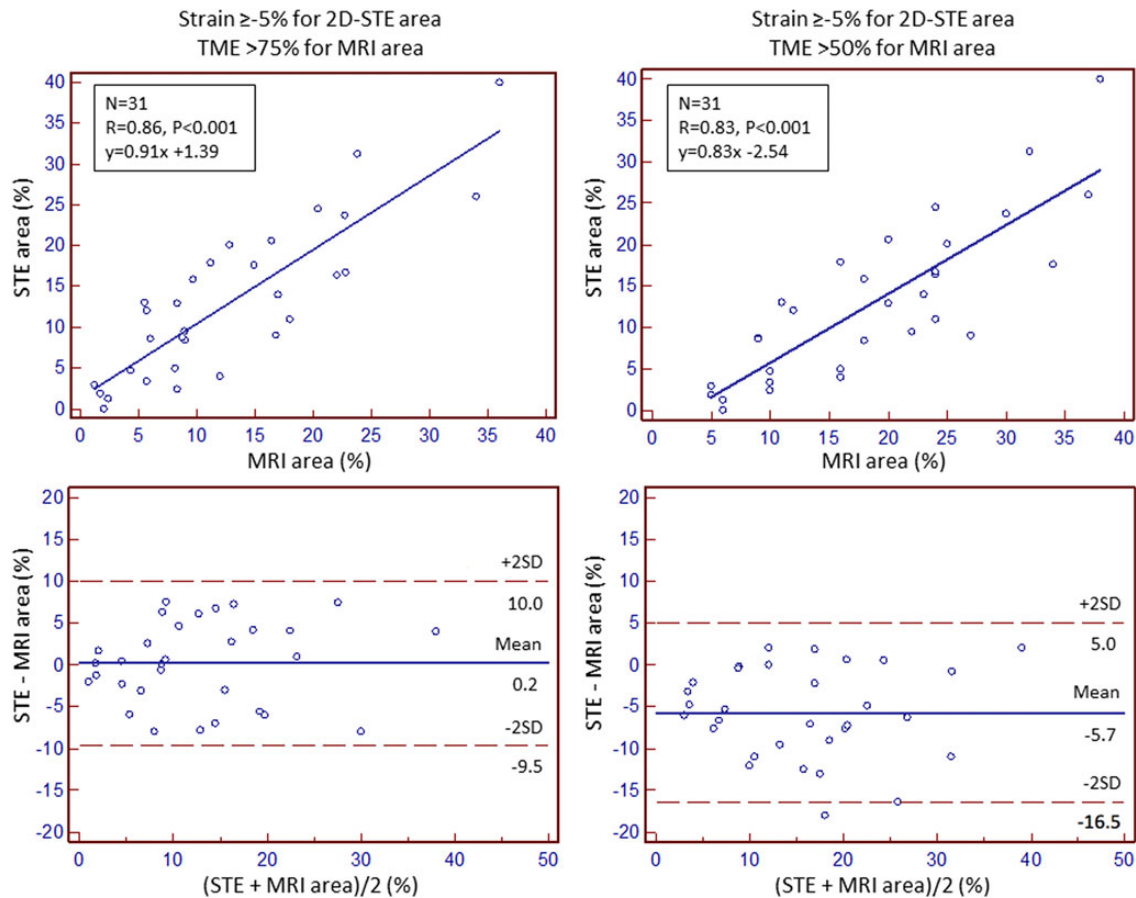


Figure 3 Regression (top) and the Bland–Altman analysis (bottom) comparing the area of left ventricular transmural scar obtained by two-dimensional speckle-tracking echocardiography (2D-STE) and magnetic resonance imaging (MRI). SD, standard deviation; TME, transmural extent of delayed enhancement.

transmural scar tissue in 96.4% of all the 496 segments studied (Figure 5). The worst agreement was observed at the mid- and apical lateral segments.

Reproducibility of SAS area evaluation

For intra-observer variability, the Lin coefficient was 0.971, the ICC 0.986 (CIs: 0.971–0.993), and the limits of agreement on the Bland–Altman analysis 4, –5% (Figure 6). For inter-observer variability, the Lin coefficient was 0.964, the ICC 0.983 (CIs: 0.963–0.992), and the limits of agreement on the Bland–Altman analysis 4.2, –5.4% (Figure 6).

Other parameters of LV systolic function

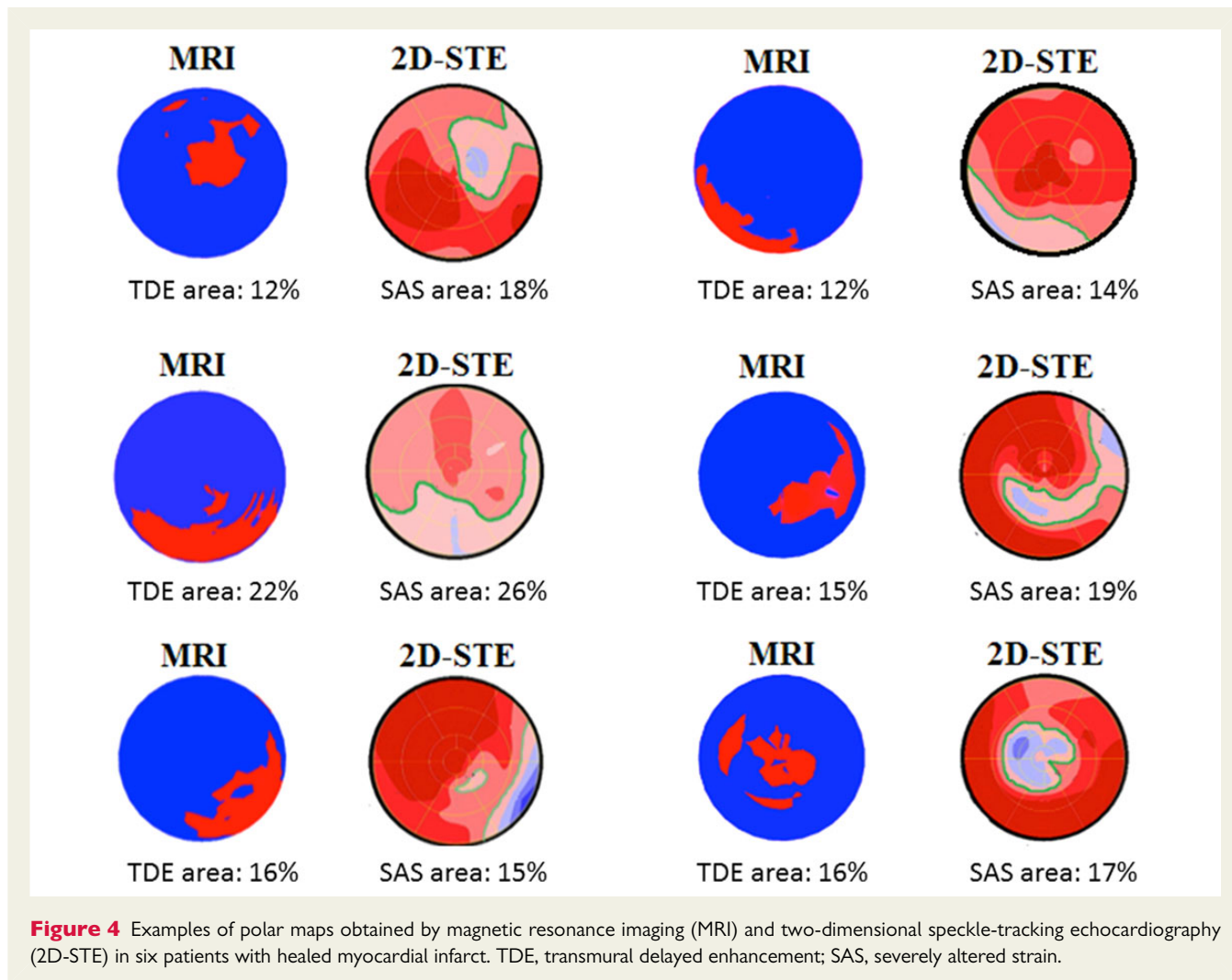
Correlations between the left ventricular ejection fraction (LV EF) and GLS values and the MRI scar areas obtained using a TME of >75% ($r = -0.35$ and 0.53 , respectively) and >50% ($r = -0.42$ and 0.60 , respectively) were lower compared with those observed using the 2D-STE SAS areas (Supplementary data online, Figure S3). On the multivariate analysis, only the 2D-STE SAS areas retained a significant correlation with the MRI scar areas both using a TME of >75% ($r = 0.77$, $P < 0.001$) and of >50% ($r = 0.74$, $P < 0.001$).

The LV EF and GLS values also correlated with the 2D-STE strain areas characterized by longitudinal strain values ≥ -5 , ≥ -10 , and ≥ -15 (Supplementary data online, Figure S4).

Patients with early and late myocardial scar evaluations

Comparison between early 2D-STE and DE-MRI

In the subgroup of 12 patients with early post-infarct 2D-STE and DE-MRI evaluations after successful revascularization, different results were obtained by the two imaging techniques. In fact, the SAS area by parametric 2D-STE was $11.8 \pm 7.2\%$ and the TDE area by MRI was $20.3 \pm 8.6\%$ ($P < 0.001$), with a correlation coefficient of $r = 0.77$ ($P = 0.004$, Figure 7); on the Bland–Altman analysis, a significant mean difference was observed (8.5%, $P < 0.001$ vs. 0), indicating a consistent overestimation by DE-MRI (Figure 7). The percentage of myocardial mass with oedema was $32.1 \pm 10.3\%$ at the MRI examination. Mean values of the peak systolic longitudinal strain in the 25 myocardial segments with oedema and non-transmural scar tissue were different from those of the 28 segments with oedema and transmural scar tissue ($-10.5 \pm 2.5\%$ vs. $0.1 \pm 4.6\%$, $P < 0.001$).



Downloaded from by guest on August 24, 2015

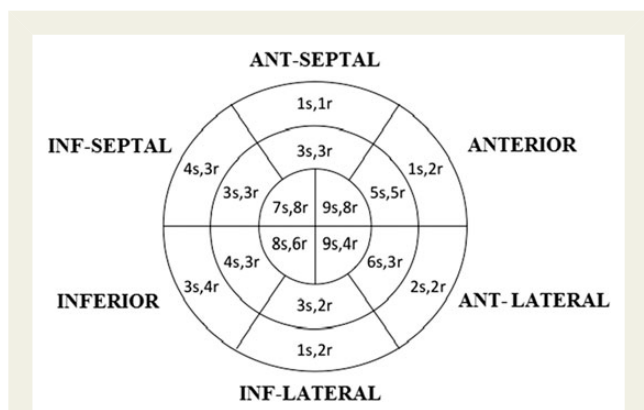


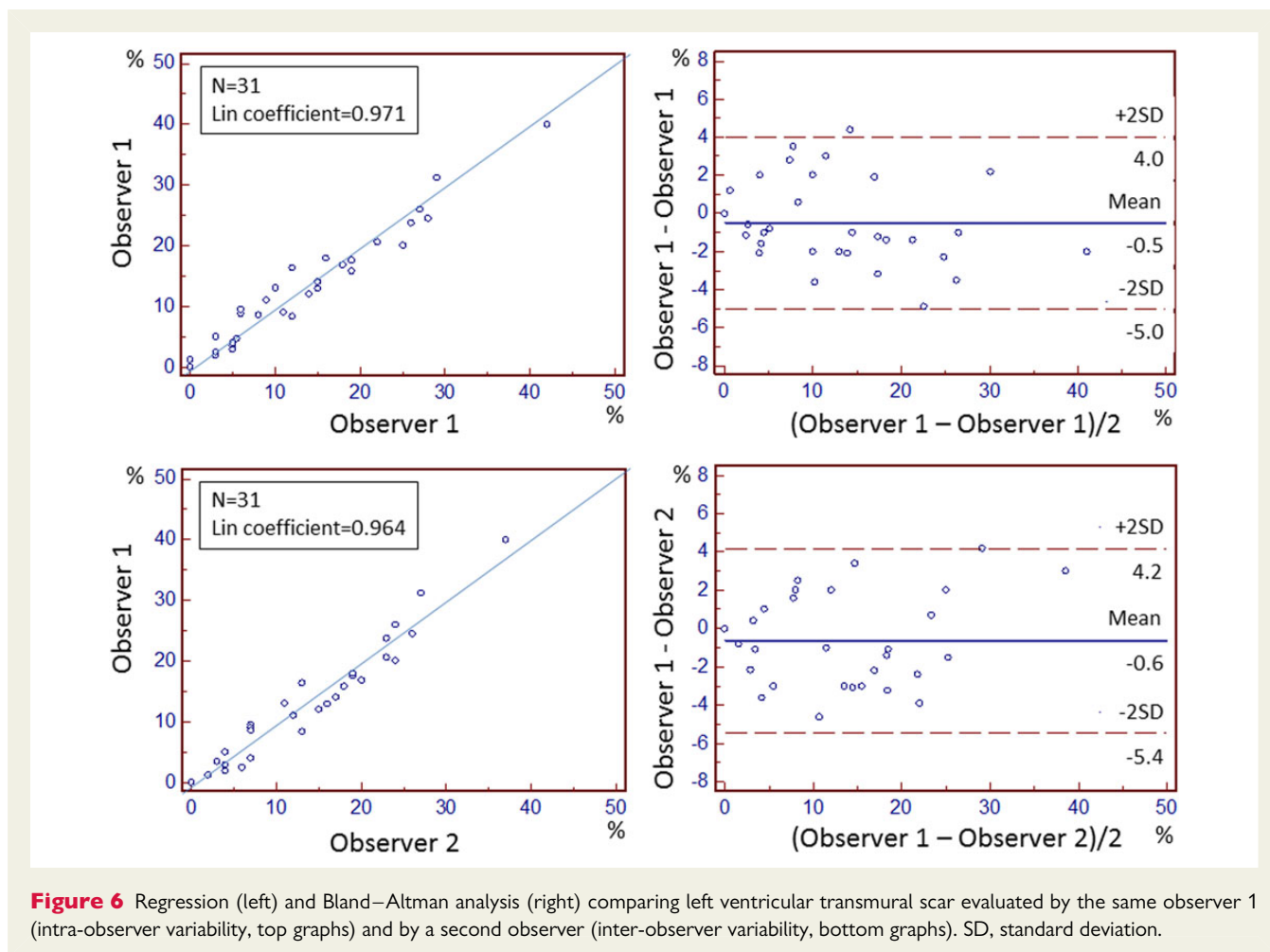
Figure 5 Bull's eye plot of the left ventricle. For each one of the 16 myocardial segments, the number of segments with transmural scar tissue identified by speckle-tracking echocardiography (s) and magnetic resonance imaging (r) is indicated. Ant, anterior; Inf, inferior.

Prediction of late transmural infarct size

On the 6-month MRI, the TDE area decreased to $14.7 \pm 8.4\%$ ($\Delta = 5.6\%$ in mean absolute reduction; $P = 0.0013$ vs. early evaluation); no residual myocardial oedema was observed. The 2D-STE SAS area was $11.6 \pm 7.0\%$ showing no difference with the early post-infarct evaluation ($\Delta = 0.2\%$ in mean absolute value, $P = 0.883$). Correlations between early 2D-STE SAS areas and MRI TDE areas with the 6-month MRI TDE areas were 0.91 ($P < 0.001$) and 0.86 ($P < 0.001$), respectively (Figure 7). At the bivariate analysis, both the early SAS and TDE areas maintained their predictive value ($P = 0.005$ and 0.049 , respectively), although the significance level was borderline for the TDE area.

Discussion

This study shows that the SAS area obtained by parametric 2D-STE of LV longitudinal strain allows accurate recognition, localization, and quantification of non-viable transmural scar tissue in comparison with cardiac MRI in patients with chronic ischaemic heart disease.



Conversely, LV GLS and EF do not seem to be helpful in this regard. Our data also show that the SAS area evaluated early after acute MI is associated to the final size of the transmural scar tissue after 6 months.

Speckle-tracking echocardiography for scar transmurality

2D-STE has the capability to perform the analysis of myocardial deformation in different spatial directions, that is, longitudinal, circumferential, and radial.^{2–4} At present, it is still unclear what is the best 2D-STE approach for the identification of healed transmural scar tissue. Authors who compared LV myocardial deformation in different spatial directions reported that circumferential^{3,4,7} and radial strain^{4,7} are better than longitudinal strain for the differentiation of scar transmurality. However, these observations should be weighed in the light of a number of considerations. First, some of these authors⁷ evaluated acute and others^{3,4} chronic MI in different patient populations. Secondly, circumferential and radial strains are based on the analysis of LV short-axis views, which is limited by non-optimal feasibility and reproducibility.^{8,9} Third, although radial and circumferential strain can potentially be evaluated in three standard short-axis views, in practice this is not always possible; thus this deformation analysis is generally restricted to only one short-axis plane. Indeed, in all the above-mentioned studies evaluating circumferential and radial strain in comparison with longitudinal

deformation,^{2–4,7} only a single, mid-ventricular short-axis view of the LV was used, with lack of strain information relative to the basal and apical portions of the LV. Finally, the predictive value of radial strain by 2D-STE for the recognition of transmural scar tissue on cardiac MRI has recently been reported to be low.¹⁰

In our study, we selected the analysis of longitudinal deformation by 2D-STE mainly because of two reasons. First, feasibility and reproducibility of longitudinal strain by 2D-STE are high, even in patients with LV systolic dysfunction,¹¹ and are better than those of circumferential and radial strain.^{3,8,9,12–16} This is fundamental to assuring an extensive clinical application of the method. Secondly, a parametric polar map of the entire LV can be easily obtained by 2D-STE using the longitudinal strain approach, since the three standard apical views needed for the 2D-STE analysis span the LV myocardium from the base to the apex of six ventricular walls. Such a polar plot representation cannot be obtained by the 2D-STE software using the radial and circumferential strain values.

Transmural scar tissue in healed MI patients

Cardiac MRI

Selection of the appropriate percentage of transmurality within the LV wall on cardiac MRI is of fundamental importance to define a segment with a transmural myocardial scar. Kaandorp *et al.*¹⁷ showed

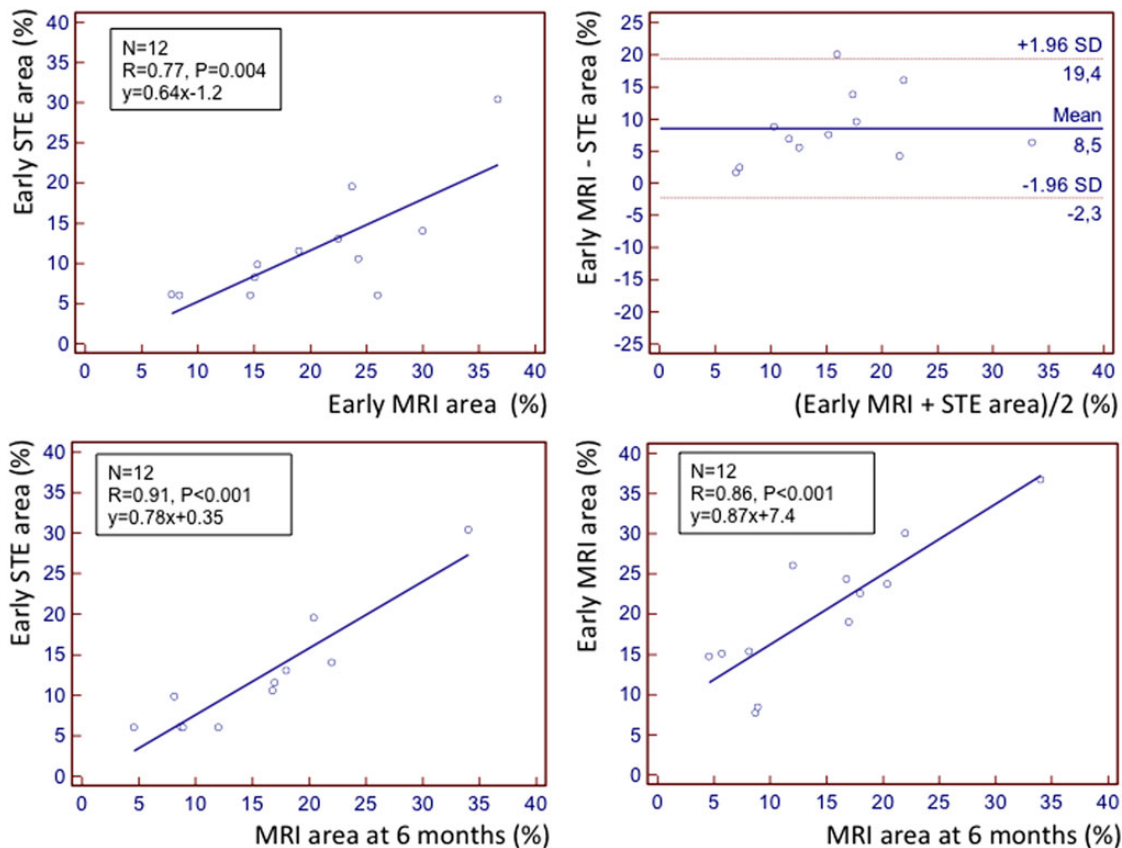


Figure 7 Regression and Bland–Altman analysis comparing the area of left ventricular transmural scar obtained by speckle-tracking echocardiography (STE) and magnetic resonance imaging (MRI). Top: early STE vs. early MRI. Bottom: early STE and MRI vs. MRI at 6 months. SD, standard deviation.

that, when scar transmural is between 50 and 75% of the myocardial wall, a large amount of LV segments still have contractile reserve, whereas when the TME is $>75\%$, contractile reserve is not frequent. Therefore, according to this observation, in our study a TME value $>75\%$ was chosen to identify scar transmural on cardiac MRI. We also explored the effect of selecting a value of $>50\%$ for scar transmural on MRI because this approach has been used in many other studies.^{1,3–5,7} In this case we observed, at the Bland–Altman analysis, a worse agreement between the SAS area evaluated by 2D-STE and the MRI scar area, with a significant mean error of -5.7% (Figure 3).

2D-STE

Our findings in patients with healed MI indicate that, using a strain cut-off value of -5% , longitudinal strain analysis by parametric 2D-STE is accurate for a comprehensive evaluation of transmural scar tissue (size and topographic distribution). This strain cut-off value is in agreement with the results of the study of Roes et al.,⁵ who showed, using the same echo scanner and software for strain analysis, that a regional longitudinal strain value of -4.5% could distinguish a transmural from a non-transmural MI with a sensitivity of 81.2% and a specificity of 81.6% in comparison with contrast MRI. Unlike our study, however, that of Roes et al.⁵ used a TME $>50\%$ at the MRI to identify

non-viable dysfunctional myocardial segments. Nevertheless, the majority (53%) of the 373 non-viable segments examined by Roes et al. had a hyperenhancement extending from 76 to 100%.⁵ We have also explored the effect of selecting a cut-off value of -10 and -15% for longitudinal strain analysis. Doing so, we observed that parametric 2D-STE markedly overestimated the MRI scar area using both a TME >75 and $>50\%$ (Supplementary data online, Figures S1 and S2). Therefore, in our patient population a longitudinal strain cut-off value of -5% showed the best capability to discriminate viable from non-viable transmural scar tissue.

Comparison with other indices of LV function

In our patient group with healed MI, the LV GLS by 2D-STE and the EF by MRI correlated worse than the SAS area by 2D-STE with the extension of the MRI scar tissue determined using both a TME >75 and $>50\%$ (Supplementary data online, Figure S3); also, the GLS and EF correlations were not significant at the multivariate analysis. This result can be apparently surprising but can be explained considering that both GLS and EF: (i) depend also on areas of viable myocardium with non-transmural scars; (ii) include normally contracting regions or even hyperkinetic or hypertrophic myocardial segments which may compensate for akinetic regions. This is confirmed in our study

by the correlations observed between the LV EF and GLS values and the 2D-STE strain areas obtained using longitudinal strain values ≥ -5 , ≥ -10 , and $\geq -15\%$ (Supplementary data online, Figure S4): there is a progressive improvement of the correlations with the progressive inclusion in the 2D-STE strain area of more myocardium with different degree of systolic dysfunction.

Early and late evaluation of infarct size

Our data show that the TDE area at cardiac MRI decreased significantly from its early evaluation after the acute MI to the 6-month evaluation. This is consistent with previous observations¹⁸ and may be explained by the infarct-associated oedema in the acute phase, which comprises a larger volume than collagenous scar tissue in the chronic phase. In support of this mechanism, we have documented that in our patients a conspicuous myocardial oedema was present acutely, which disappeared completely at the 6-month evaluation.

The SAS area measured by 2D-STE early after the acute MI did not vary significantly at 6 months. Also, this early 2D-STE SAS area was associated with late transmural infarct area on cardiac MRI better than the early MRI TDE area (Figure 7). These observations are in accordance with previous findings of a good relationship between strain in acute MI and chronic infarct size.¹⁹

Although in our patients parametric 2D-STE of LV longitudinal strain showed to be a valuable technique for early prediction of non-viable MI tissue, some consideration should be made to avoid data overinterpretation. First, we only examined 12 patients with both early and 6-month evaluations. Secondly, systolic strain in acute/early MI can be affected by myocardial oedema, because incompressibility of the oedema may reduce myocardial deformation.

Advantages of parametric polar plot maps

The use of parametric polar plot maps of longitudinal strain obtained by 2D-STE has additional advantages over the utilization of strain curves (longitudinal, radial, and circumferential) because polar maps: (i) are generated semi-automatically; (ii) avoid measurements on strain curves, which can be tedious and generally require more expertise; (iii) allow immediate spatial appreciation of the dysfunctioning myocardial tissue, thus facilitating the visual analysis of the LV myocardial deformation even by cardiologists who are not expert in the interpretation of strain curves. It should also be considered that the strain curves used in previous investigations^{2–5,7} represent the average strain value of myocardial segments and therefore include both the viable and non-viable myocardial tissue which may be present in each segment. Conversely, parametric polar plot maps precisely identify the regions with non-viable myocardial tissue only.

Study limitations

(i) A relatively small patient population was studied. This, however, may be balanced by the high feasibility and reproducibility of the 2D-STE technique used in this study to assess longitudinal myocardial strain. (ii) Analysis of myocardial deformation at the level of the mid- and apical lateral wall can sometimes be problematic, because of reduced speckle-tracking quality. This may explain the non-optimal concordance for transmural scar location between 2D-STE and MRI which was observed in some patients at the level of the mid–apical lateral wall. (iii) Three-dimensional STE may

theoretically overcome some limitations of 2D-STE, such as the through-plane motion; however, this technique has not been used in this study because it is not yet recommended for clinical practice and its real reproducibility has not been clearly established. (iv) Measurements of both MRI and 2D-STE areas of non-viable myocardium were relative and not based on calibrated units; however, relative measures are also quantitative and comparable to each other. (v) Finally, this study was not designed to provide information about the discrimination of transmural from non-transmural healed MIs, which might be the object of a specific investigation.

Conclusions

Parametric 2D-STE of LV longitudinal strain is a feasible, reproducible, and accurate technique for recognition, localization, and quantification of non-viable transmural scar tissue in patients with chronic ischaemic heart disease. Possible applications can be the study of LV remodelling and cardiac resynchronization therapy.

Supplementary data

Supplementary data are available at *European Journal of Echocardiography* online.

Conflict of interest: None declared.

References

- Kim RJ, Wu E, Rafael A, Chen EL, Parker MA, Simonetti O *et al.* The use of contrast-enhanced magnetic resonance imaging to identify reversible myocardial dysfunction. *N Engl J Med* 2000;**343**:1445–53.
- Becker M, Hoffmann R, Kühl HP, Grawe H, Katoh M, Kramann R *et al.* Analysis of myocardial deformation based on ultrasonic pixel tracking to determine transmural-ity in chronic myocardial infarction. *Eur Heart J* 2006;**27**:2560–6.
- Chan J, Hanekom L, Wong C, Leano R, Cho GY, Marwick TH. Differentiation of subendocardial and transmural infarction using two-dimensional strain rate imaging to assess short-axis and long-axis myocardial function. *J Am Coll Cardiol* 2006;**48**:2026–33.
- Rost C, Rost MC, Breithardt OA, Schmid M, Klinghammer L, Stumpf C *et al.* Relation of functional echocardiographic parameters to infarct scar transmural-ity by magnetic resonance imaging. *J Am Soc Echocardiogr* 2014;**27**:767–74.
- Roes SD, Mollema SA, Lamb HJ, van der Wall EE, de Roos A, Bax JJ. Validation of echocardiographic two-dimensional speckle tracking longitudinal strain imaging for viability assessment in patients with chronic ischemic left ventricular dysfunction and comparison with contrast-enhanced magnetic resonance imaging. *Am J Cardiol* 2009;**104**:312–7.
- Heiberg E, Sjogren S, Ugander M, Carlsson M, Engblom H, Arheden H. Design and validation of segment-freely available software for cardiovascular image analysis. *BMC Med Imaging* 2012;**10**:1.
- Sjoli B, Örn S, Grenne B, Ihlen H, Edvardsen T, Brunvand H. Diagnostic capability and reproducibility of strain by Doppler and by speckle tracking in patients with acute myocardial infarction. *JACC Cardiovasc Imaging* 2009;**2**:24–33.
- Villanueva-Fernández E, Ruiz-Ortiz M, Mesa-Rubio D, Ortega MD, Romo-Peñas E, Toledano-Delgado F *et al.* Feasibility of bidimensional speckle-tracking echocardiography for strain analysis in consecutive patients in daily clinical practice. *Echocardiography* 2012;**29**:923–6.
- Risum N, Ali S, Olsen NT, Jons C, Khouri MG, Lauridsen TK *et al.* Variability of global left ventricular deformation analysis using vendor dependent and independent two-dimensional speckle-tracking software in adults. *J Am Soc Echocardiogr* 2012;**25**:1195–203.
- Bakos Z, Ostenfeld E, Markstad H, Werther-Evaldsson A, Roijer A, Arheden H *et al.* A comparison between radial strain evaluation by speckle-tracking echocardiography and cardiac magnetic resonance imaging, for assessment of suitable segments for left ventricular lead placement in cardiac resynchronization therapy. *Europace* 2014;**16**:1779–86.
- Mignot A, Donal E, Zaroui A, Reant P, Salem A, Hamon C *et al.* Global longitudinal strain as a major predictor of cardiac events in patients with depressed left ventricular function: a multicenter study. *J Am Soc Echocardiogr* 2010;**23**:1019–24.

12. Eek C, Grenne B, Brunvand H, Aakhus S, Endresen K, Hol PK et al. Strain echocardiography and wall motion score index predicts final infarct size in patients with non-ST-segment-elevation myocardial infarction. *Circ Cardiovasc Imaging* 2010;**3**:187–94.
13. Gjesdal O, Helle-Valle T, Hopp E, Lunde K, Vartdal T, Aakhus S et al. Noninvasive separation of large, medium, and small myocardial infarcts in survivors of reperfused ST-elevation myocardial infarction: a comprehensive tissue Doppler and speckle-tracking echocardiography study. *Circ Cardiovasc Imaging* 2008;**1**:189–96.
14. Yingchoncharoen T, Agarwal S, Popović ZB, Marwick TH. Normal ranges of left ventricular strain: a meta-analysis. *J Am Soc Echocardiogr* 2013;**26**:185–91.
15. Cheng S, Larson MG, McCabe EL, Osypiuk E, Lehman BT, Stanchev P et al. Reproducibility of speckle-tracking-based strain measures of left ventricular function in a community-based study. *J Am Soc Echocardiogr* 2013;**26**:1258–66.
16. Manovel A, Dawson D, Smith B, Nihoyannopoulos P. Assessment of left ventricular function by different speckle-tracking software. *Eur J Echocardiogr* 2010;**11**:417–42.
17. Kaandorp TA, Bax JJ, Schuijf JD, Viergever EP, van Der Wall EE, de Roos A et al. Head-to-head comparison between contrast-enhanced magnetic resonance imaging and dobutamine magnetic resonance imaging in men with ischemic cardiomyopathy. *Am J Cardiol* 2004;**93**:1461–4.
18. Ripa RS, Nilsson JC, Wang Y, Sondergaard L, Jorgensen E, Kastrup J. Short- and long-term changes in myocardial function, morphology, edema, and infarct mass after ST-segment elevation myocardial infarction evaluated by serial magnetic resonance imaging. *Am Heart J* 2007;**154**:929–36.
19. Vartdal T, Brunvand H, Pettersen E, Smith HJ, Lyseggen E, Helle-Valle T et al. Early prediction of infarct size by strain Doppler echocardiography after coronary reperfusion. *J Am Coll Cardiol* 2007;**49**:1715–21.